



Evaluation of Given Dose Accuracy in Radiation Therapy of Patient with Breast Cancer Using Diode In Vivo Dosimetry

Sepideh Rasouli Farah¹, Ahmad Mostaar ^{1,*}, Ahmad Ameri², Ahmad R Mafi ² and Robab Anbiaee²

¹Department of Medical Physics and Biomedical Engineering, School of Medicine, Shahid Beheshti University of Medical Science, Tehran, Iran

²Department of Radiation Oncology, Imam Hossein Hospital, School of Medicine, Shahid Beheshti University of Medical Science, Tehran, Iran

*Corresponding author: Department of Medical Physics and Biomedical Engineering, School of Medicine, Shahid Beheshti University of Medical Science, Tehran, Iran. Email: mostaar@sbmu.ac.ir

Received 2020 September 21; Revised 2021 January 12; Accepted 2021 January 16.

Abstract

Background: The main goal of radiation therapy is to deliver the highest dose to the tumor and at the same time the lowest dose to the surrounding normal tissue. In vivo dosimetry is a quality control procedure that, instead of controlling the components separately, directly examines the dose reached to the tumor area.

Objectives: In this study, the entrance, exit, and middle dose of the breast and supraclavicular area of patients with breast cancer under radiation therapy were measured and compared with calculations.

Methods: In this experimental study, the entrance and exit doses of 33 patients with breast tumors treated with 6 MV and 18MV photons were measured simultaneously. The measurement was done, using p-type diodes after calibration and, then, the midpoint dose was calculated, using the transfer method and arithmetic mean method. Also, the entrance dose, exit dose, and midline dose measured with dosimeter were compared with the calculated values in the treatment planning system.

Results: There was no significant difference between calculated and measured doses in the entrance, exit, and midline point in breast regions ($P > 0.05$), but in the supraclavicular region, a challenge was observed. The difference in entrance and midline point between calculation and measurement is not significant based on the transfer method, but there is a significant error based on the arithmetic mean method ($P < 0.05$).

Conclusions: In vivo dosimetry by measured real given dose to the patient can perform a basic role in the quality control of the radiotherapy department. It seems in the entrance dose, the relative error is smaller but due to the smaller value of exit dose, the relative error in small values is more apparent.

Keywords: Radiation Therapy, Breast Cancer, In Vivo Dosimetry, Diode Detector, Quality Control

1. Background

Cancer is one of the leading causes of mortality in industrialized and advanced societies, with breast cancer being the most common malignancy in women worldwide and accounting for about one-third of all female cancers. Breast cancer is the second most common cancer after lung cancer, which is increasing in Iranian women (1). Elimination of malignant cells using the effect of ionizing radiation on living tissue is one of the most effective methods in the treatment of cancerous tumors (2). Among different medical applications, radiation therapy has the highest level of radiation exposure. Therefore, the use of such radiation levels without consideration, along with the undeniable role of radiation therapy, can have painful clinical outcomes. National and international organizations such as the International Atomic

Energy Agency (IAEA), International Commission on Radiation Units and Measurements (ICRU), and American Association of Physicists in Medicine (AAPM) have put forward strategies to prevent possible events and to achieve desired therapeutic outcomes, including modifying structures, setting limits for uncertainties, and quality control programs (3-5). In radiation therapy, the goal is to transfer the maximum dose to the tumor so that healthy tissues around the dose receive the minimum dose (6, 7). According to the World Protocol, only $\pm 5\%$ of treatment uncertainties are allowed, indicating the need to carefully monitor the dose and control it to improve the quality of treatment. The only viable way to ensure the accuracy of treatment and control the actual dose delivered to the patient is an in vivo dosimetry that empirically checks the correct dose delivered to the patient during treatment and if any discrepancies are found, it can be resolved before

treatment is continued (3, 8-10). Various detectors such as a diode, thermoluminescence dosimeter (TLD), MOSFET, film dosimeter, as well as electronic portal imaging systems are used for in vivo dosimetry (8, 11-14). Diode properties such as immediate response, high sensitivity to radiation, high mechanical strength, small and simple, robust and independent of air pressure and availability in medical centers make them a more suitable choice for in vivo dosimetry (12, 13, 15-17).

2. Objectives

This study aims at performing in vivo dosimetry, using diode semiconductor detectors in the treatment of patients with breast cancer in the Radiotherapy Department of Imam Hossein Hospital in Tehran to determine the amount of error at the end of each treatment session. For this purpose, the entrance dose, exit dose, and middle dose of the breast and supraclavicular (SC) area of 33 patients with breast cancer under radiation therapy were measured and compared with calculations.

3. Methods

In this experimental study, for measurement of dose, two semiconductor detectors with T60010MP serial number for 5 - 13 MV photons and two semiconductor detectors with T60010HP serial number for 13 - 25 MV photons were employed. These semiconductor detectors are of p-type silicon, which is connected to a PTW-MUTIDOS T10004 multichannel electrometer simultaneously by an accessories diode ceiling mount system. In addition, a 0.6cc Farmer ionization chamber made by PTW-Freiburg TM30010 model with PTW-UNIDOS T10001 electrometer was used as a reference detector to determine calibration factors and correction factors. Also, the RWS slab phantom with dimensions of $30 \times 30 \text{ cm}^2$ in the thickness of 1, 2, 5, and 10 mm T40006 model made by the PTW factory was used to determine the calibration and correction factors. The accelerator used was the American-made Varian linear accelerator 2300C/D model. Also, in this regard, VivoSoft software (PTW-Freiburg, GmbH) was used to obtain calibration factors and correction coefficients and doses of entrance and exit points of patients in vivo, as well as Monte Carlo simulation algorithm to determine the midline dose of patients by transfer method. To convert the read number from the diode in the electrometer to the absorption dose and also to perform a high-precision in vivo dosimetry, the calibration of the diodes was done. Diode calibration was performed in two steps:

The first step was calibration under reference conditions to determine the calibration factors of detectors and

the second step was the calibration to obtain the correction factors when the measurement conditions were different from the reference conditions.

In the measurements to avoid the shadow effect, the entrance diode was placed 2 cm away from the central axis of radiation on the phantom surface (18). The reproducibility of the diode was tested after calibration and the variation responses were less than 0.5%. The temperature dependency was not considered because of (a) small differences between the calibration temperature and measurement temperature, (b) layer of epoxy resin beneath the diodes that delays the transfer of body heat to the diode over a 2 to 3 minute period of measurement, and (c) small temperature dependency for the diode that was used in this study (about 0.1% per°C).

3.1. Determination of the Calibration Factors Entrance and Exit

The in vivo semiconductor probes were placed on the surface of the slab phantoms by the calibration adapter "S" so that the thickness of the slab phantoms and the thickness of the adapter in the position of the probe was a total of 15 cm. The Farmer ionization chamber was placed in the central axis beam in the maximum depth dose; this depth is 1.5 cm for the 6 MV photon beam and 3.3 cm for the 18 MV photon beam. The radiation conditions close to the treatment conditions were set to field sizes $10 \times 10 \text{ cm}^2$ and SSD = 100 cm. The head of the Linac was placed at a zero-degree angle, in which the central axis of radiation was perpendicular to the phantom surface. The entrance diodes and ionization chamber were, then, irradiated once by a 6 MV photon beam and again by an 18 MV photon beam for a given time. The calibration factor for each energy was, then, determined separately as the ratio of the absorption dose measured by the ionization chamber at the maximum depth dose to the semiconductor signal in reference conditions.

For exit conditions, only the head of the Linac was rotated 180 degrees to radiate from the bottom of the phantom. In this case, only the source surface distance (SSD) setting from the bottom to the phantom level was set to 100 cm. The calibration factor for each energy was, then, calculated separately.

The detector entrance and exit dose calibration factors, F_{en} , and F_{ex} are given by (19-23):

$$F_{en} = \left[\frac{D_{en}}{M_{en}} \right] \quad (1)$$

$$F_{ex} = \left[\frac{D_{ex}}{M_{ex}} \right] \quad (2)$$

Where D_{en} and D_{ex} are measured by the ion chamber, and M_{en} and M_{ex} are responses of the entrance and exit semiconductor detectors. For this purpose, dosimetry protocol IAEA TRS-398 for determination of dose by ion chamber and VivoSoft software for assigning dose to diodes were used. In Figure 1A, the diode system and Linac that was used in this study were illustrated and in Figure 1B, setup for determination of the calibration factor for entrance point by ion chamber was shown.

3.2. Determination of Correction Factors

Correction factors are required when the measurement conditions are different from the reference conditions. In this study, correction factors were determined for SSD, field sizes, and radiant angles.

Slab phantoms were used to determine these correction factors. The diodes were placed at the surface of the phantom and the ion chamber was placed at the maximum depth dose. To determine the SSD correction factor, with a $10 \times 10 \text{ cm}^2$ field size at SSDs of 85, 90, 95, 100, and 10^5 cm , the ionization chamber and the diode were irradiated simultaneously for a certain monitor unit (MU). The reference SSD was 100 cm. Also, to determine the field size correction factor, the ionization chamber and diodes were irradiated simultaneously for a given MU by changing the field size ($5 \times 5, 8 \times 8, 10 \times 10, 12 \times 12, 15 \times 15, 18 \times 18, 20 \times 20 \text{ cm}^2$) at a constant SSD (100 cm). The reference field size was $10 \times 10 \text{ cm}^2$. The SSD and field size correction factors were determined by Equation 3 (16, 18, 23, 24):

$$CF_{SSD, FS} = \frac{\left[\frac{D_{ic}}{R_{diode}} \right]_{mea}}{\left[\frac{D_{ic}}{R_{diode}} \right]_{ref}} \quad (3)$$

Where $\left[\frac{D_{ic}}{R_{diode}} \right]_{mea}$ is the ratio of the dose measured by the ionization chamber and the semiconductor detector reading for the different SSD under the measurement conditions and $\left[\frac{D_{ic}}{R_{diode}} \right]_{ref}$ is the ratio of the dose measured by the ionization chamber and the semiconductor detector reading for the SSD value in the reference condition.

Slab phantoms were used to determine the angle correction factor. The diodes were placed at the surface of the phantom. In addition to the radiation angle, the radiation conditions were adjusted to the reference conditions. The change in diode response with different radiation angles was determined for angles 0, 30, 60, 330, 300 degrees. In this case, at a constant time, the reading rate of the diode was obtained with different radiation angles. The angle correction factors are determined as (23, 25):

$$CF_{arc} = \frac{R(\theta)}{R(\theta_{cal})} \quad (4)$$

Where $R(\theta)$ is the diode reading for different angles and $R(\theta_{cal})$ is the diode reading for the calibration angle (zero degrees angle).

3.3. Entrance and Exit Dose Measurement

Before irradiation, diode detectors were placed on the patient's skin, in the central axis of the radiation, at the entrance and exit of the beam. To avoid the shadow effect, the entrance diode 2 cm away from the center of the radiation field, and the exit diode in the center of the radiation field was glued to the skin with anti-allergy glue. After irradiation, the readings of the diodes were read online. Measured entrance dose and exit doses by the diode were calculated, using the following equations (6, 19, 20, 26-28):

$$D_{en} = M_{en} \cdot F_{en} \cdot CF_{en}^{SSD} \cdot CF_{en}^{FS} \cdot CF_{en}^{angle} \quad (5)$$

$$D_{ex} = M_{ex} \cdot F_{ex} \cdot CF_{ex}^{SSD} \cdot CF_{ex}^{FS} \cdot CF_{ex}^{angle} \quad (6)$$

Where M_{en} and M_{ex} are the amounts of entrance and exit diode reading, F_{en} and F_{ex} are the entrance and exit calibration factor, CF_{en}^{SSD} , CF_{en}^{FS} , and CF_{en}^{angle} are the entrance dose correction factors for SSD, field size, and angle of radiation, respectively, and CF_{ex}^{SSD} , CF_{ex}^{FS} , and CF_{ex}^{angle} are the exit dose correction factors for SSD, field size, and angle of radiation, respectively.

3.4. Middle Dose Estimation

The best way to determine the amount of dose at the midpoint is to place the dosimeter directly inside the body at the target point. In most cases, it is not possible to place the dosimeter inside the body. For this purpose, various methods have been proposed to determine the amount of dose at the midpoint. In this study, the transfer method and the arithmetic mean method have been used. The middle of the line between the input and output points was considered the midpoint.

In the arithmetic mean method, the middle point dose ($D_{midline}$) is estimated from the average dose of the entrance and exit points obtained by in vivo dosimeter (21, 29, 30).

In the transfer method, the simulation algorithm was used, using the Monte Carlo code. For this purpose, a homogeneous cubic water phantom with dimensions of $15 \times 30 \times 30 \text{ cm}^3$ was designed in the algorithm. The head of the accelerator was considered at a zero degree angle and the field size was $10 \times 10 \text{ cm}^2$ and SSD = 90 cm. The codes were performed once for the 6 MV photon beam and once for the 18MV photon beam. Then, doses for the 6 MV photon beam were calculated at a depth of 1.5 cm (maximum depth



Figure 1. A, Illustration of diode system and Linac for in vivo dosimetry; B, Setup for determination of the calibration factor for entrance point by ion chamber

dose) from the entrance level, at the midpoint of the phantom. Also, doses for 18 MV photon beam were calculated at a depth of 3.3 cm from the input surface (maximum depth dose), at the midpoint of the phantom. After measuring the entrance (D_{en}), exit (D_{ex}), and middle doses (D_{mid}) of a phantom, the coefficients of intermediate transfer rate (T_{mid}) were calculated as follows (21):

$$T_{mid(en)} = D_{mid}/D_{en} \quad (7)$$

Thus, with the entrance dose (D_{en}) measured by the diode and by the use of the intermediate transfer rate (T_{mid}), the middle dose was obtained from the following equations (31-33):

$$D_{midline} = D_{en} \times T_{mid(en)} \quad (8)$$

3.5. Data Analysis

To evaluate the purpose of this study that is an investigation of agreement between the given dose and the treat-

ment planning system calculations, the calculated dose of the entrance, exit, and middle points (D_{cal}) from the treatment planning system was extracted and compared with the measured values (D_{meas}) in the same points. The treatment planning system was Isogray (Dosisoft Company) and dose calculation was done by collapsed cone convolution (CCC) algorithm.

The analysis of results was done, using Equation 9 based on the percentage deviation of the measured dose from the calculated dose. The SPSS (ver.16, Chicago IL, USA) software was used for statistical analysis. For a value of $P \leq 0.05$, the difference was assumed to be statistically significant. For this purpose, the K-S method was used to investigate the normal distribution of data and to check the significance of the measured dose deviation from the calculated dose, the paired-sample t test, and Wilcoxon methods were used.

$$\begin{aligned} & \text{Deviation of measured dose from calculated dose (\%)} \\ & = (D_{meas} - D_{cal}) / D_{cal} \times 100 \end{aligned} \quad (9)$$

4. Results

4.1. Calibration Factors of Diode Detectors

Calibration of diodes was performed to determine the absorption dose at the input and output points of the phantom. The values of input and output calibration factors are given in [Table 1](#).

4.2. Field Size Correction Factor

The variations of field size correction factor for entrance and exit points as a function of field size for diode detectors T60010MP-4 model and T60010HP-8 model at the entrance point for 6 MV and 18 MV photon beams and for diode detector T60010MP-5 model and T60010HP-9 model in the exit points for 6 MV and 18 MV photon beams are shown in [Figure 2](#). These field size correction factors are normalized to the value of $10 \times 10 \text{ cm}^2$ field size for each diode model.

4.3. SSD Correction Factors

The variations of SSD correction factor for entrance and exit points as a function of SSD for diode detector T60010MP-4 model and T60010HP-8 model at the entrance point for 6 MV and 18 MV photon beams and diode detector T60010MP-5 model and T60010HP-9 model in the exit points for 6 MV and 18 MV photon beams are shown in [Figure 3](#). These SSD correction factors are normalized to the value of 100 cm SSD for each diode model.

4.4. Angle Correction Factor

The changes of the angle correction factor for different angles (from 60 to 300 degrees) for diode detector T60010MP-4 model and T60010HP-5 model for 6 MV photon beam and diode detector T60010MP-8 model and T60010HP-9 model for 18 MV photon beam are displayed in [Figure 4](#). The values are normalized to zero degrees as the reference condition.

4.5. Comparison of Measured Dose and Calculated Dose

The percentage of deviation of the measured dose from the calculated dose for the entrance and exit points of the breast and SC region is shown in [Table 2](#).

The differences between measured dose and calculated dose based on the transfer method showed a normal distribution with an average of 0.48% and standard deviation of $\pm 4.7\%$ for breast area as shown in [Figure 5](#) and average

of -0.61% and standard deviation of $\pm 4.39\%$ for SC area as shown in [Figure 6](#).

Also, the differences between measured dose and calculated dose based on the arithmetic mean method showed a normal distribution with an average of 0.51% and standard deviation of $\pm 2.12\%$ for breast area as shown in [Figure 7](#) and average of -3.54% and standard deviation of $\pm 2.83\%$ for SC area as shown in [Figure 8](#).

5. Discussion

Regarding the effect of field size on the entrance and exit points as shown in [Figure 2](#), by increasing the field, the correction factor for the entrance and exit points for photon 6MV and 18MV increases at first and reaches an almost constant value from field size $12 \times 12 \text{ cm}^2$ onwards. The entrance diode located on the phantom surface is slightly affected by the scattered of the phantom to determine the correction factor, while it is completely dependent on the scattered from the linac head. Considering the relationship (3), the change in the correction factor with the field size is due to the different sensitivity of the diode and the ionization chamber to the scattered photons and average energy. Since the response of the diode depends on the radiant energy but the response of the ionization chamber is almost energy-independent, if the dimensions of the field increase, the energy spectrum increases, and the scatter photons inside the linac head are added to the beam. As a result, the average energy of the beam decreases, and the response of the diode differs from the ion chamber. For the field size correction factor at the exit point by increasing the field size, in addition to the scattered beam, the scattered beam from the phantom increased and this effect is more valuable. These results are in good agreement with Yaparpalvi et al. (34) that reported confirmation of dose for breast cancer with diode, Huang et al. (35) that reported characteristics of the diode for clinical use, and Rodríguez et al. that reported Isorad diodes on patients of pelvic cancer (18).

Changing the response of diodes with radiant angles, the maximum change of the measured ratios for diodes is about 4%. The response of the diode to the radiant angle was investigated by Yaparpalvi et al. and the result for the diode was about 2% for angles greater than 60 and about 1.5% for angles less than 60. The reason for the differences could be due to the directional dependence of the diodes on the shape and structure of the diode (34).

The results of the one-sample Kolmogorov-Smirnov test showed that the diagram of the percentage of relative deviation for the measured input, output, and middle doses from the calculated dose for the breast area ($P = 0.2$) and the SC area ($P = 0.2$) has a normal distribution.

Table 1. Results of Calibration Factors for Different Diode Detectors

Semiconductor Detectors	Color and Energy Range	Entrance Calibration Factor (mGy/nC)	Exit Calibration Factor (mGy/nC)
T60010MP-4	Yellow, 5 – 13 MV	5.327×10^6	-
T60010MP-5	Yellow, 5 – 13 MV	-	5.725×10^6
T60010HP-8	Red, 13 – 25 MV	3.374×10^6	-
T60010HP-9	Red, 13 – 25 MV	-	4.359×10^6

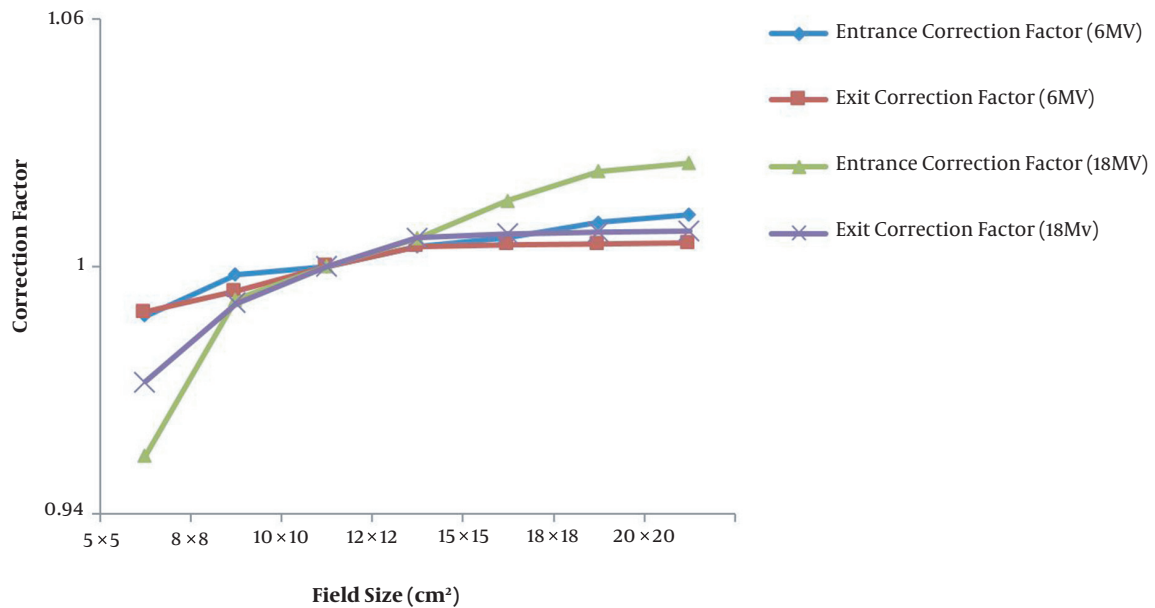


Figure 2. Field size correction factor for entrance and exit diode types for 6 MV and 18 MV photon beams

Table 2. Deviation of Measured Dose from a Calculated Dose as a Percentage for Entrance, Exit, and Midpoint Dose

	Average Deviation (%)	Standard Deviation (%)	Error Greater than ± 5 (%)
Entrance dose of tangent fields	0.47	± 3.1	13.63
Exit dose of tangent fields	0.62	± 3.82	25.75
Midpoint dose of breast (transfer method)	0.48	± 4.7	39.39
Midpoint dose of the breast (arithmetic mean method)	-0.51	± 2.12	3.03
Entrance dose of SC fields	0.56	± 2.58	10.81
Exit dose of SC fields	-0.51	± 3.84	21.26
Midpoint dose of SC (transfer method)	-0.61	± 4.34	25.81
Midpoint dose of SC (arithmetic mean method)	-3.54	± 2.82	35.45

5.1. Measuring the Dose at the Entrance Point

The results of the paired-sample t test showed no significant difference between the measured and calculated input dose of the breast area ($P = 0.32$), but there was a significant difference for the SC area ($P = 0.032$). The relative difference greater than $\pm 5\%$ can be seen in 13.63% of the

breast entrance dose and 10.81% of the SC entrance dose. In radiation therapy of breast cancer with the SAD technique, some errors can happen such as an error in patient positioning setup or adjusting treatment parameters. Histogram analysis of the input dose showed that the mean error and standard deviation is 0.47% ($\pm 3.1\%$) for the breast

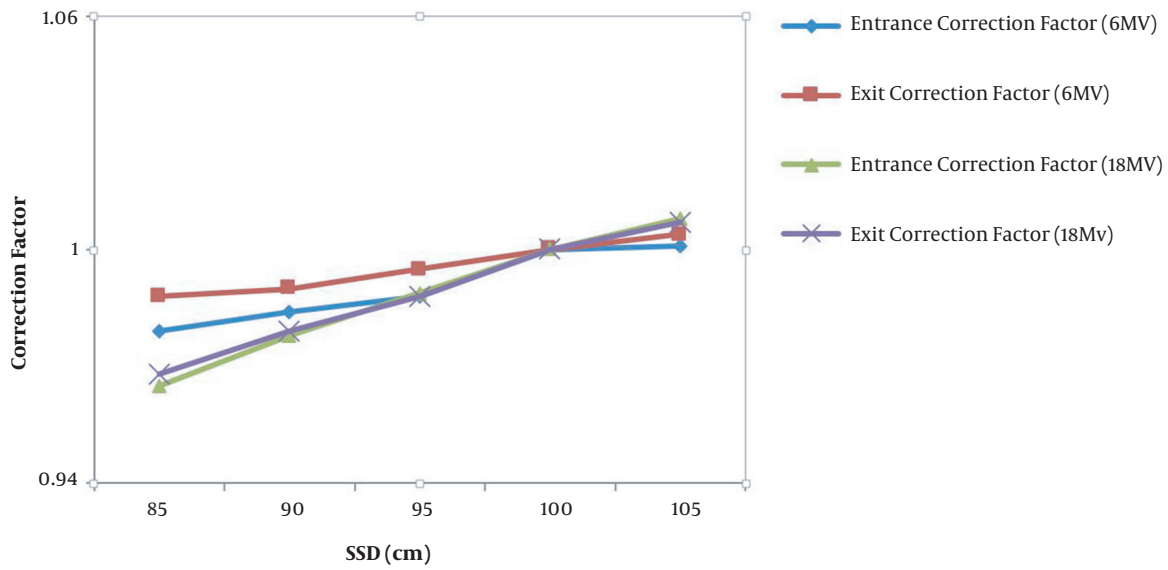


Figure 3. SSD correction factor for entrance and exit diode types for 6MV and 18MV photon beams

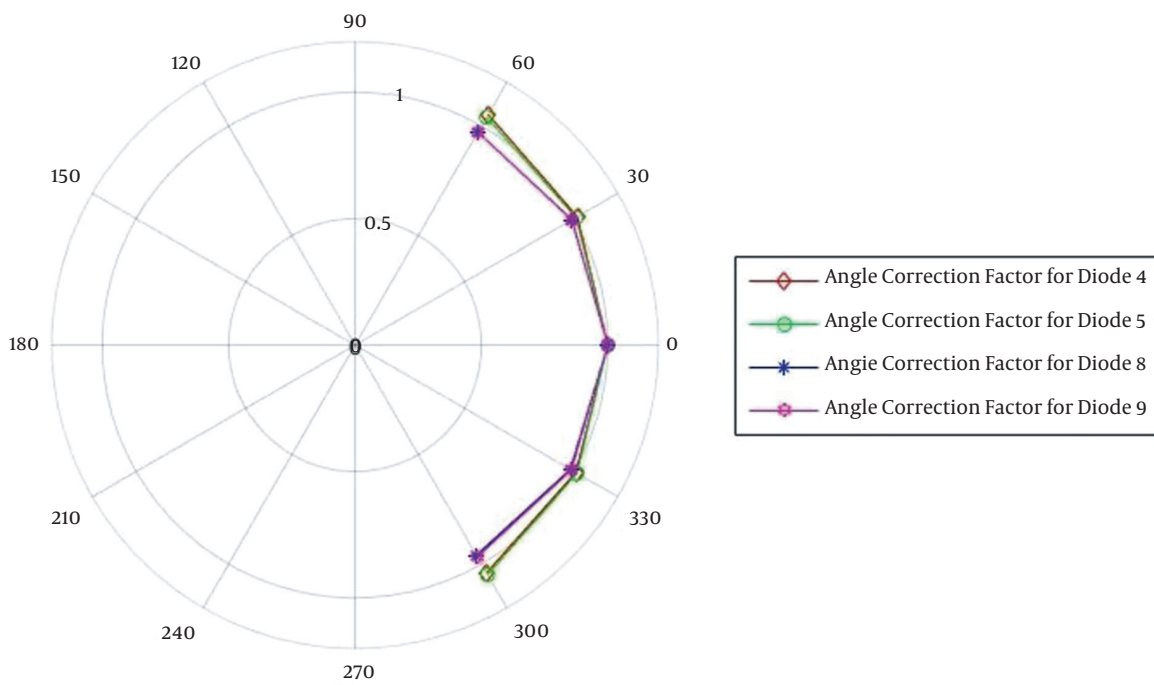


Figure 4. Angle correction factor for different diode detectors

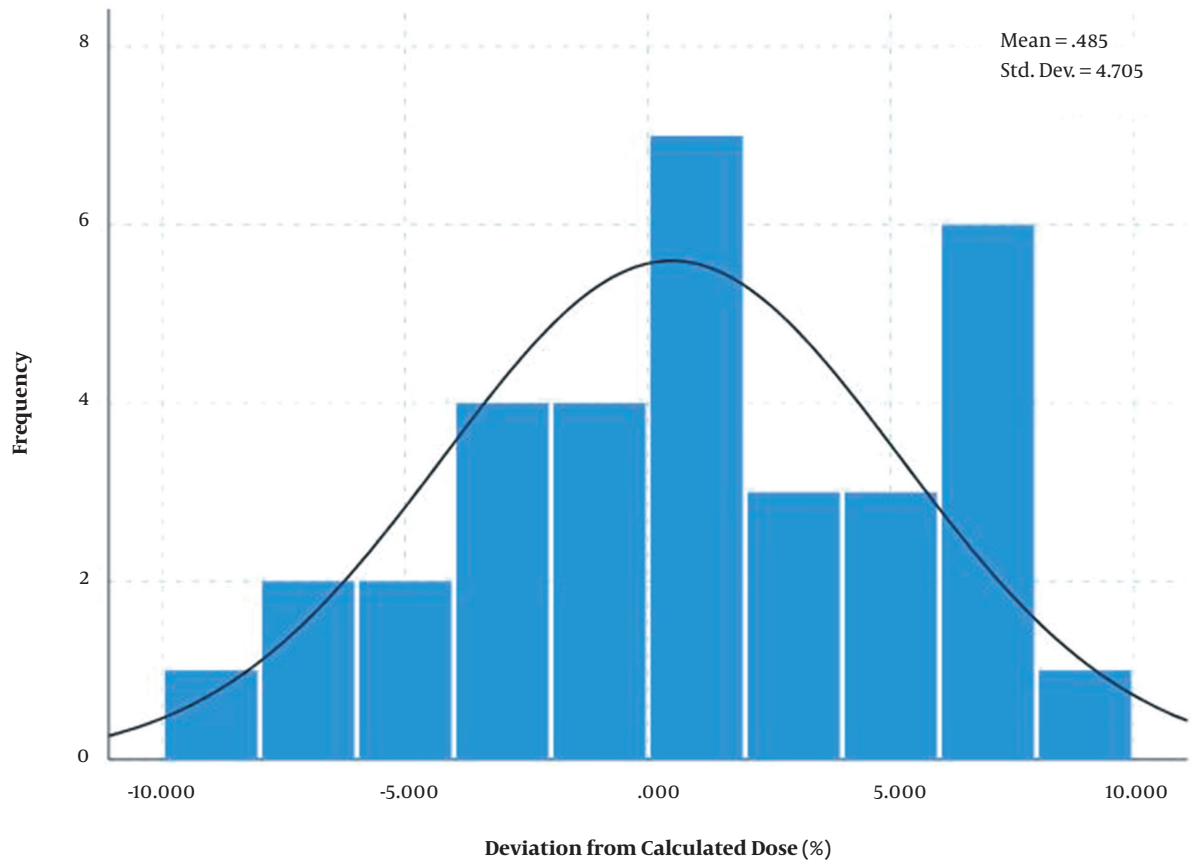


Figure 5. Percentage deviation of estimated middle dose from calculated dose based on transfer method for the breast region

area and 0.56% ($\pm 2.58\%$) for the SC area. The results indicate that the error in the breast area at the entry point is greater and wider than in the SC area. This can be due to the curvature of the breast tissue, as well as the instability of the breast tissue, which can lead to errors in SSD adjustment and patient positioning. The errors observed in the supraclavicular region can be due to the placement of the bed and breast board in the path of radiation entering the body in the posterior field and defective TPS in applying the appropriate absorption coefficient. Also, the errors can be due to the diode not being in the proper position at the point of entry of the posterior field due to not seeing the optical field. Also, in the SAD breast treatment technique, the SSD is first fixed to the anterior field and, then, the gantry is rotated for posterior irradiation without changing the SSD, thus increasing the contour error in the posterior field for the entry point. Besides, in the fields of the supraclavicular area, due to the shielding of the humerus bone in patients and the use of trays to hold the shield,

these trays have different absorption coefficients, which are all considered with the same absorption coefficient in the treatment planning system and this can cause errors in measuring entrance dose.

In 1998, Voordeckers et al. performed in vivo dosimetry on the entrances of various patients and reported a relative deviation for patients with breast cancer more than other patients, which was consistent with the results of this project (36). Also, in 2012, Vasile et al. achieved a relative deviation with a mean and standard deviation of -0.6% ($\pm 2.208\%$) during in vivo dosimetry with diodes at the entrance points of patients undergoing breast cancer treatment with 6MV and 25MV photons and reported that most of these errors probably due to SSD differences and the detector being in the wrong position (37). In general, measuring the input dosage by the in vivo dosimetry method is useful for detecting errors in checking and confirming the system such as patient setup and beam parameters, output and operation of the machine, as well as data transmis-

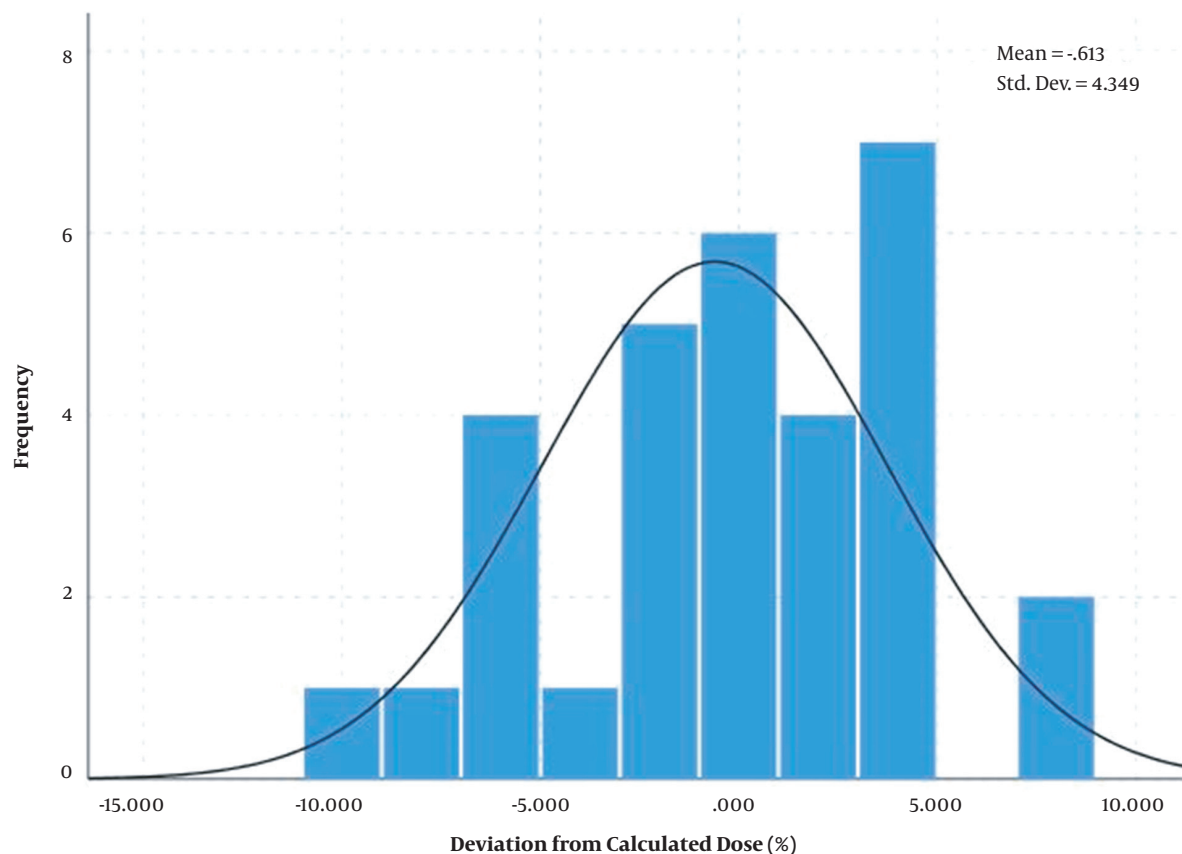


Figure 6. Percentage deviation of estimated middle dose from calculated dose based on transfer method for SC region

sion that should be corrected for the next session before treatment. Errors greater than 10% can be due to the patient's movement (voluntary or involuntary) and the lack of proper diode installation.

5.2. Measuring the Dose at the Exit Point

The results of the paired-sample t test showed no significant difference between the measured and calculated output dose of the breast area ($P = 0.067$) and the SC area ($P = 0.565$). The relative difference greater than $\pm 5\%$ can be seen in 25.75% of the breast exit dose and 21.62% of the SC exit dose. Histogram analysis of the output dose showed that the mean error and standard deviation is 0.62% ($\pm 3.82\%$) for the breast area and -0.51% ($\pm 3.84\%$) for the SC area. The error at the exit point of the breast area can be due to the curvature of the breast tissue, which results in an error in adjusting the SSD and adjusting the patient's position, which affects the output point dose. The errors observed in the supraclavicular region can be due to the

placement of the diode in the wrong position at the point of the output of the anterior field, placement of the bed and breast board in the beam path at the point of the output of the posterior field, and passing the beam through the tray used to protect the head of the humerus in the anterior field. Also, in the SAD breast treatment technique, the SSD is first fixed to the anterior field and, then, the gantry is rotated for posterior irradiation without changing the SSD, thus increasing the contour error in the posterior field for the output point.

In general, measuring the output dose by the in vivo dosimeter method can be useful for detecting errors related to the patient's contour, changing the patient's thickness, which may be due to swelling, contraction, or tissue analysis. It is also possible to obtain information about the amount of heterogeneity in the path of the beam, although the impact of heterogeneity is largely taken into account in the new TPS systems, it cannot be said that the

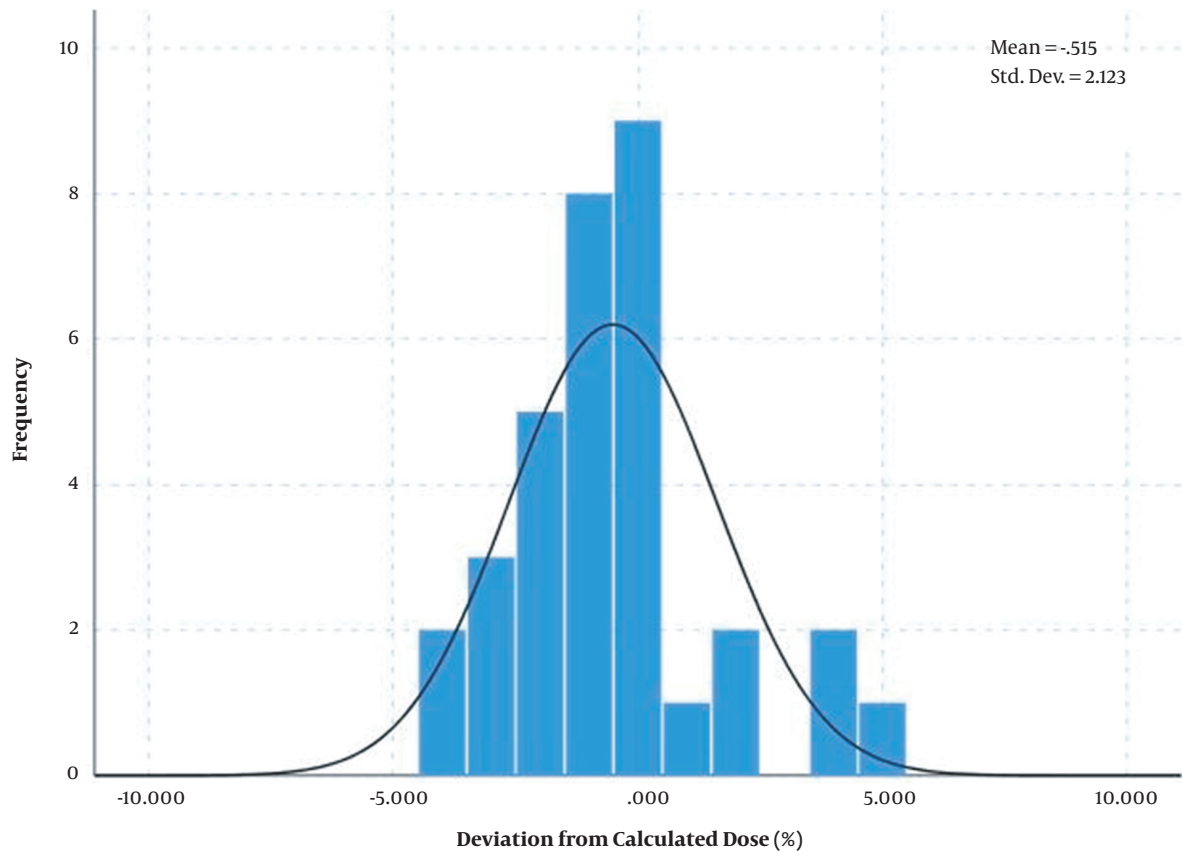


Figure 7. Percentage deviation of estimated middle dose from calculated dose based on the arithmetic mean method for the breast region

effect of heterogeneity is completely considered because this effect varies from one computational algorithm to another. According to the results obtained in all fields and patients, the extent of deviation of the outlet from the input is greater than the calculated dose, which can be because the non-uniformity, curvature, and density of the tissue have less effect on the input point, while beam after passing through the breast tissue, undergoes more changes due to non-uniformity, curvature, the density of the breast tissue and the diameter of the transient tissue, and as a result, it deviates more than the calculated dose. This is consistent with the results of Strojnik since the wider spread of exit dose deviations (SD 3.3%) was reported in comparison to the entrance dose deviations (SD 2.1%) in patients with rectal cancers (38).

5.3. Estimating the Dose at the Middle Point

The results of the paired-sample t test showed no significant difference between the measured and calculated middle dose based on the transfer method for the breast

area (P = 0.439) and the SC area (P = 0.436). In 1996, Yarpalvi et al. (34) used the transfer rate algorithm to calculate the midpoint dose of patients with breast cancer and concluded that the midline dose corresponded to the expected dose for all patients. Rodríguez et al. (18) used the same algorithm to calculate the midpoint dose of pelvic patients and did not report a significant difference between the measured and calculated values.

The results of the paired-sample t test showed no significant difference between the measured and calculated middle dose based on the arithmetic method for the breast area (P = 0.159), but there was a significant difference for the SC area (P = 0.001). It seems that the arithmetic means algorithm for the breast region can be a suitable substitute for the transfer rate method in estimating the midpoint dose. The appropriateness of the arithmetic means algorithm for determining the midpoint dose for the breast region is recommended in a study conducted by Allahverdi and Vaezzadeh in 2010 (32).

Considering that there is no significant difference be-

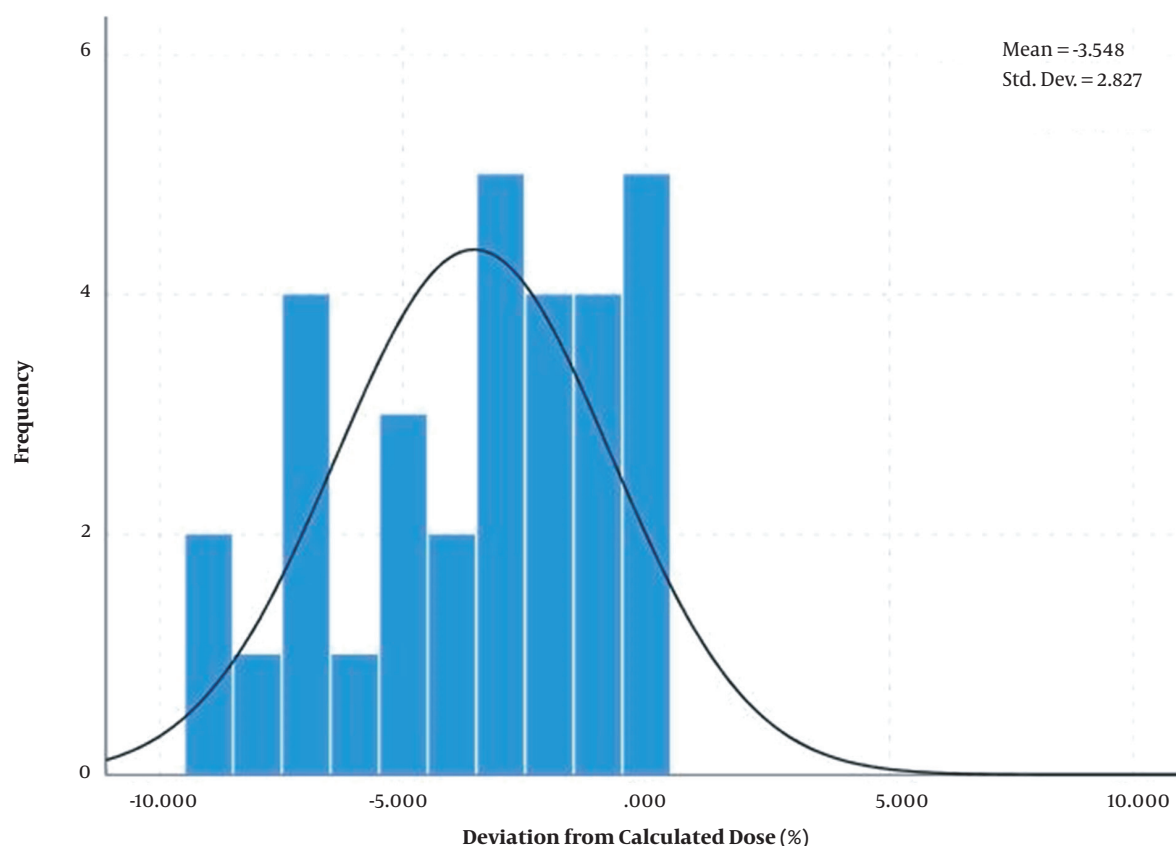


Figure 8. Percentage deviation of estimated middle dose from calculated dose based on the arithmetic mean method for SC region

tween the calculated and measured midpoint dose in the breast region in both methods, the result of this study can be reported with more certainty. However in the supraclavicular region, because the results of the two methods are not the same, there may be differences that can be due to the placement of the bed and breast board in the path of radiation entering the body in the posterior fields and tray plate for the anterior fields, which TPS is defective in applying the appropriate absorption coefficient.

Comparison of the standard deviation between the input, output, and center point histograms shows the highest bandwidth at the output point and the next level the midpoint, and the lowest bandwidth at the input point. The reasons for this discrepancy, as previously explained, could be due to differences in the thickness of the heterogeneities, the contour error, and the curvature. Also, the amount of dose decreases with the passage of the tissue, and the relative errors are apparent more in small amounts. This is consistent with the findings of Rodríguez et al. and Yaparalvi et al. (18, 34).

5.4. Conclusions

In vivo dosimetry, as part of quality control, can be useful for examining and evaluating all the therapeutic chains of a radiotherapy department, and the errors that are far from the eye and the errors that occur in the treatment can be detected. Errors seen at the end of treatment can be caused by systematic or accidental errors and occur from various sources, including errors in calibration and correction factors, patient adjustment, equipment and devices, patient contouring, data transmission, computational algorithms, device output, patient movement, and individual errors were noted. Of course, errors need to be evaluated in separate fields as well, because the total error may be within the allowable range, but errors in a separate field may be too permissible to be considered. Errors from separate fields may compensate for each other and mislead our total error.

The results of this study show that in the breast area, despite the errors mentioned above, the dose delivered to the breast tumor is not significantly different from the ex-

pected dose. In the supraclavicular region, there was no significant difference between the delivered dose and the expected dose according to the transfer method, but there was a significant difference according to the arithmetic mean method; it seems that the cause of the error may be larger and a significant error may occur. Therefore, to reduce these errors based on the results of this study, it is recommended due to the absorption in the immobilization devices and the treatment bed, in the techniques that the radiation field passes through these devices, their effect on the given dose should be considered. Also for shielded fields, each center must use the trays by the same absorption coefficient.

Acknowledgments

This study has been extracted from the MSc thesis of Mrs. Sepideh Rasouli Farah at the medical physics field in the School of Medicine, Shahid Beheshti University of Medical Science (Registration No:20161).

Footnotes

Authors' Contribution: Study concept and design: Sepideh Rasouli Farah, Ahmad Mostaar and Ahmad R Mafi; Acquisition of data: Sepideh Rasouli Farah and Ahmad Mostaar; Statistical analysis: Sepideh Rasouli Farah and Ahmad Mostaar; Analysis and interpretation of data: Ahmad Ameri, Ahmad R Mafi and Robab Anbiaee; Drafting of the manuscript: Sepideh Rasouli Farah and Ahmad Mostaar; Study supervision: Ahmad Mostaar; All authors approved the final version of the manuscript.

Conflict of Interests: There was no conflict of interest to be declared.

Ethical Approval: The Ethical Committee of Shahid Beheshti University of Medical Sciences approved this study (Ethical code: IR.SBMU.MSP.REC.1398.585).

Funding/Support: The authors received no financial support for the research, authorship, and/or publication of this article.

Informed Consent: It was not declared by authors.

References

- Behdad A, Mahdizadeh M, Yazdi F, Hosseinpour M. Demographic and clinical characteristics of the women with breast complaints. *Yafteh*. 2001;3(9):41-4.
- Hall EJ, Giaccia AJ. *Radiobiology for the Radiologist*. 8th ed. LWW; 2018.
- Noel A, Aletti P, Bey P, Malissard L. Detection of errors in individual patients in radiotherapy by systematic in vivo dosimetry. *Radiation Oncol*. 1995;34(2):144-51. doi: [10.1016/0167-8140\(94\)01503-u](https://doi.org/10.1016/0167-8140(94)01503-u). [PubMed: 7597213].
- Menzel H. International Commission on Radiation Units and Measurements. *JICRU*. 2014;14(2):1-2. doi: [10.1093/jicru_ndx006](https://doi.org/10.1093/jicru_ndx006).
- Blyth C, McLeod AS, Thwaites DI. A pilot study of the use of in vivo diode dosimetry for quality assurance in radiotherapy. *Radiography*. 1997;3(2):131-42. doi: [10.1016/s1078-8174\(97\)90018-3](https://doi.org/10.1016/s1078-8174(97)90018-3).
- Essers M, Lanson JH, Mijnheer BJ. In vivo dosimetry during conformal therapy of prostatic cancer. *Radiation Oncol*. 1993;29(2):271-9. doi: [10.1016/0167-8140\(93\)90258-a](https://doi.org/10.1016/0167-8140(93)90258-a).
- Leunens G, Verstraete J, Van den Bogaert W, Van Dam J, Dutreix A, van der Schueren E. Human errors in data transfer during the preparation and delivery of radiation treatment affecting the final result: "garbage in, garbage out". *Radiation Oncol*. 1992;23(4):217-22. doi: [10.1016/s0167-8140\(92\)80124-2](https://doi.org/10.1016/s0167-8140(92)80124-2).
- Jornet N, Carrasco P, Jurado D, Ruiz A, Eudaldo T, Ribas M. Comparison study of MOSFET detectors and diodes for entrance in vivo dosimetry in 18 MV x-ray beams. *Med Phys*. 2004;31(9):2534-42. doi: [10.1118/1.1785452](https://doi.org/10.1118/1.1785452). [PubMed: 15487735].
- Dutreix A. When and how can we improve precision in radiotherapy? *Radiation Oncol*. 1984;2(4):275-92. doi: [10.1016/s0167-8140\(84\)80070-5](https://doi.org/10.1016/s0167-8140(84)80070-5).
- Kutcher GJ, Coia L, Gillin M, Hanson WF, Leibel S, Morton RJ, et al. Comprehensive QA for radiation oncology: report of AAPM Radiation Therapy Committee Task Group 40. *Med Phys*. 1994;21(4):581-618. doi: [10.1118/1.597316](https://doi.org/10.1118/1.597316). [PubMed: 8058027].
- Yekta ZR, Mahdavi SRM, Baghani HR, Robotjazi M, Mostaar A, Mirzaie H, et al. In vivo dosimetry using radiochromic films (EBT-2) during intraoperative radiotherapy. *J Radiation Pract*. 2016;15(4):378-84. doi: [10.1017/s1460396916000273](https://doi.org/10.1017/s1460396916000273).
- Essers M, Mijnheer B. In vivo dosimetry during external photon beam radiotherapy. *Int J Radiat Oncol Biol Phys*. 1999;43(2):245-59. doi: [10.1016/s0360-3016\(98\)00341-1](https://doi.org/10.1016/s0360-3016(98)00341-1).
- Van Dam J, Leunens G, Dutreix A. Correlation between temperature and dose rate dependence of semiconductor response; influence of accumulated dose. *Radiation Oncol*. 1990;19(4):345-51. doi: [10.1016/0167-8140\(90\)90035-u](https://doi.org/10.1016/0167-8140(90)90035-u).
- Kroonwijk M, Pasma KL, Quint S, Koper PC, Visser AG, Heijmen BJ. In vivo dosimetry for prostate cancer patients using an electronic portal imaging device (EPID); demonstration of internal organ motion. *Radiation Oncol*. 1998;49(2):125-32. doi: [10.1016/s0167-8140\(98\)00122-4](https://doi.org/10.1016/s0167-8140(98)00122-4).
- Jursinic PA. Implementation of an in vivo diode dosimetry program and changes in diode characteristics over a 4-year clinical history. *Med Phys*. 2001;28(8):1718-26. doi: [10.1118/1.1388217](https://doi.org/10.1118/1.1388217). [PubMed: 11548942].
- Marre D, Marinello G. Comparison of p-type commercial electron diodes for in vivo dosimetry. *Med Phys*. 2004;31(1):50-6. doi: [10.1118/1.1630492](https://doi.org/10.1118/1.1630492). [PubMed: 14761020].
- Meigooni AS, Sowards K, Myron G. Evaluation of the veridose in vivo dosimetry system. *Medical Dosimetry*. 2002;27(1):29-36. doi: [10.1016/s0958-3947\(02\)00085-7](https://doi.org/10.1016/s0958-3947(02)00085-7).
- Rodriguez ML, Abrego E, Pineda A. Implementation of in vivo dosimetry with Isorad semiconductor diodes in radiotherapy treatments of the pelvis. *Med Dosim*. 2008;33(1):14-21. doi: [10.1016/j.meddos.2007.04.004](https://doi.org/10.1016/j.meddos.2007.04.004). [PubMed: 18262118].
- Alecu R, Alecu M, Ochran TG. A method to improve the effectiveness of diode in vivo dosimetry. *Med Phys*. 1998;25(5):746-9. doi: [10.1118/1.598237](https://doi.org/10.1118/1.598237). [PubMed: 9608486].
- Cozzi L, Fogliata-Cozzi A. Quality assurance in radiation oncology. A study of feasibility and impact on action levels of an in vivo dosimetry program during breast cancer irradiation. *Radiation Oncol*. 1998;47(1):29-36. doi: [10.1016/s0167-8140\(97\)00202-8](https://doi.org/10.1016/s0167-8140(97)00202-8).
- Tung CJ, Wang HC, Lo SH, Wu JM, Wang CJ. In vivo dosimetry for external photon treatments of head and neck cancers by diodes and TLDS. *Radiat Prot Dosimetry*. 2004;111(1):45-50. doi: [10.1093/rpd/nch358](https://doi.org/10.1093/rpd/nch358). [PubMed: 15367767].
- Lanson JH, Essers M, Meijer GJ, Minken AWH, Uiterwaal GJ, Mijnheer BJ. In vivo dosimetry during conformal radiotherapy. *Radiation Oncol*. 1999;52(1):51-9. doi: [10.1016/s0167-8140\(99\)00074-2](https://doi.org/10.1016/s0167-8140(99)00074-2).

23. York E, Alecu R, Ding L. *AAPM Report No. 87*. American Association of Physicists in Medicine, College Park, MD; 2005.
24. Fontenla DP, Yaparalvi R, Chui C, Briot E. The use of diode dosimetry in quality improvement of patient care in radiation therapy. *Medical Dosimetry*. 1996;**21**(4):235–41. doi: [10.1016/s0958-3947\(96\)00081-7](https://doi.org/10.1016/s0958-3947(96)00081-7).
25. Allahverdi M. *Accuracy in radiotherapy dosimetry [Thesis]*. University of Edinburgh; 1998.
26. Yaparalvi R, Fontenla DP, Vikram B. Clinical experience with routine diode dosimetry for electron beam radiotherapy. *Int J Radiat Oncol Biol Phys*. 2000;**48**(4):1259–65. doi: [10.1016/s0360-3016\(00\)00763-x](https://doi.org/10.1016/s0360-3016(00)00763-x).
27. Greene S, Price RA. Energy and angular anisotropy optimisation of a p-type diode for in vivo dosimetry in photon-beam radiotherapy. *Radiat Prot Dosimetry*. 2005;**116**(1-4 Pt 2):152–9. doi: [10.1093/rpd/nci021](https://doi.org/10.1093/rpd/nci021). [PubMed: [16604618](https://pubmed.ncbi.nlm.nih.gov/16604618/)].
28. Verney JN, Morgan AM. Evaluation of in vivo dose measurements for patients undergoing electron boost treatments. *Radiother Oncol*. 2001;**59**(3):293–6. doi: [10.1016/s0167-8140\(01\)00323-1](https://doi.org/10.1016/s0167-8140(01)00323-1).
29. Millwater CJ, MacLeod AS, Thwaites DI. In vivo semiconductor dosimetry as part of routine quality assurance. *Br J Radiol*. 1998;**71**(846):661–8. doi: [10.1259/bjr.71.846.9849391](https://doi.org/10.1259/bjr.71.846.9849391). [PubMed: [9849391](https://pubmed.ncbi.nlm.nih.gov/9849391/)].
30. Nilsson B, Rudén B, Sorcini B. Characteristics of silicon diodes as patient dosimeters in external radiation therapy. *Radiother Oncol*. 1988;**11**(3):279–88. doi: [10.1016/0167-8140\(88\)90011-4](https://doi.org/10.1016/0167-8140(88)90011-4).
31. Allahverdi M, Taghizadeh MR. [Achievable accuracy in brain tumors by in vivo dosimetry with diode detectors]. *Int J Radiat Res*. 2006;**3**(4):153–61. Persian.
32. Allahverdi M, Vaezzadeh SA. Verification of dose accuracy delivered to the tumors of pelvis region and breast cancer by in vivo dosimetry method using semiconductor dosimeter. *Radiother Oncol*. Elsevier Science Ireland Ltd., Elsevier House, Brookvale Plaza East Park Shannon, Co; 2010. p. S493–4.
33. Rizzotti A, Compri C, Garusi GF. Dose evaluation to patients irradiated by 60Co beams, by means of direct measurement on the incident and on the exit surfaces. *Radiother Oncol*. 1985;**3**(3):279–83. doi: [10.1016/s0167-8140\(85\)80036-0](https://doi.org/10.1016/s0167-8140(85)80036-0).
34. Yaparalvi R, Fontenla DP, Yu L, Lai PP, Vikram B. Radiation therapy of breast carcinoma: confirmation of prescription dose using diodes. *Int J Radiat Oncol Biol Phys*. 1996;**35**(1):173–83. doi: [10.1016/s0360-3016\(96\)85027-9](https://doi.org/10.1016/s0360-3016(96)85027-9).
35. Huang K, Bice WJ, Hidalgo-Salvatierra O. Characterization of an in vivo diode dosimetry system for clinical use. *J Appl Clin Med Phys*. 2003;**4**(2):132–42. doi: [10.1120/jacmp.v4i2.2528](https://doi.org/10.1120/jacmp.v4i2.2528). [PubMed: [12777148](https://pubmed.ncbi.nlm.nih.gov/12777148/)]. [PubMed Central: [PMC5724474](https://pubmed.ncbi.nlm.nih.gov/PMC5724474/)].
36. Voordeckers M, Goossens H, Rutten J, Van den Bogaert W. The implementation of in vivo dosimetry in a small radiotherapy department. *Radiother Oncol*. 1998;**47**(1):45–8. doi: [10.1016/s0167-8140\(97\)00177-1](https://doi.org/10.1016/s0167-8140(97)00177-1).
37. Vasile G, Vasile M, Dului OG. In vivo dosimetry measurements for breast radiation treatments. *Rom Rep Phys*. 2012;**64**(3):728–36.
38. Strojnik A. In vivo dosimetry with diodes in rectal cancer patients. *Radiol Oncol*. 2007;**41**(4):196–202. doi: [10.2478/v10019-007-0031-8](https://doi.org/10.2478/v10019-007-0031-8).